0026-895X/98/040712-10$3.00/0

MOLECULAR PHARMACOLOGY, **54:**712–721 (1998).

A Common Anticonvulsant Binding Site for Phenytoin, Carbamazepine, and Lamotrigine in Neuronal Na^+ Channels

CHUNG-CHIN KUO

Department of Physiology, National Taiwan University College of Medicine, and Department of Neurology, National Taiwan University Hospital, Taiwan, Republic of China

Received March 26, 1998; Accepted June 22, 1998

This paper is available online at http://www.molpharm.org

ABSTRACT

Phenytoin, carbamazepine, and lamotrigine are anticonvulsants frequently prescribed in seizure clinics. These drugs all show voltage-dependent inhibition of Na^+ currents, which has been implicated as the major mechanism underlying the antiepileptic effect. In this study, I examine the inhibition of Na^+ currents by mixtures of different anticonvulsants. Quantitative analysis of the shift of steady state inactivation curve in the presence of multiple drugs argues that one channel can be occupied by only one drug molecule. Moreover, the recovery from inhibition by a mixture of two drugs (a fast-unbinding drug plus a slow-unbinding drug) is faster, or at least not slower, than the recovery from inhibition by the slow-unbinding drug alone. Such kinetic characteristics further strengthen the argument that binding of one anticonvulsant to the Na^+ channel precludes binding of the other. It also is found that these anticonvulsants are effective inhibitors of Na^+ currents only when applied externally, not internally. Altogether these findings suggest that phenytoin, carbamazepine, and lamotrigine bind to a common receptor located on the extracellular side of the Na^+ channel. Because these anticonvulsants all have much higher affinity to the inactivated state than to the resting state of the Na^+ channel, the anticonvulsant receptor probably does not exist in the resting state. Thus, there may be correlative conformational changes for the making of the receptor on the extracellular side of the channel during the gating process.

Epilepsy is a common neurological disorder. Different types of seizures may have different neurobiological bases and are controlled with different medications. DPH and CBZ have been the mainstay in the treatment of generalized tonic-clonic and partial seizure for a few decades (Rogawski and Porter, 1990). LTG is an anticonvulsant just in clinical use that shows similar effect to DPH and CBZ when used as monotherapy in newly diagnosed epilepsy (Steiner *et al*., 1994; Brodie *et al*., 1995). LTG, CBZ, and DPH also are similar in antiepileptic profiles in animal seizure models (Miller *et al*., 1986) and in use-dependent block of neuronal discharges at the cellular level (McLean and McDonald, 1983, 1986; Lees and Leach, 1993; Xie *et al*., 1995). The use-dependent block of discharges has been considered of great mechanistic importance because it readily explains why these anticonvulsants effectively inhibit only seizure discharges and spare most normal neuronal activities.

The molecular basis underlying the use-dependent block of discharges has been ascribed to voltage-dependent inhibition of Na^+ currents. DPH, CBZ, and LTG all inhibit Na^+ currents, and the inhibition is more pronounced at more depolarized membrane potentials (Matsuki *et al*., 1984; Willow *et al*., 1985; Lang *et al*., 1993; Kuo and Bean, 1994a; Xie *et al*., 1995; Kuo and Lu, 1997; Kuo *et al*., 1997). Detailed examination of the steady state effect and reaction kinetics of DPH, CBZ, and LTG on central neuronal Na^+ currents further discloses very similar qualitative features in the molecular interactions between these anticonvulsants and the Na^+ channel (Kuo and Bean, 1994a; Kuo and Lu, 1997; Kuo *et al*., 1997). For example, these drugs all bind to the channel via a simple bimolecular reaction (a one-to-one binding process), and they all have a much higher affinity toward the fast inactivated state than toward the resting (deactivated) state of Na^+ channels.

Despite the striking similarities in the mode of action on neuronal Na^+ channels by DPH, CBZ, and LTG, the chemical structures of these drugs apparently are not similar (Fig. 1A). DPH is a hydantoin containing the ureide structure (Fig. 1B), which is traditionally viewed as an important structural motif responsible for antiepileptic activities. CBZ, however, does not contain the ureide structure and is a tricyclic compound with a very short amide side chain. LTG is an even simpler compound composed of only two aromatic rings. Could the very similar mode of action still indicate that these drugs bind to the same binding site or "receptor" in the Na^+

This work was supported by Grant NSC-86–2314-B-002–195 from National Science Council, Taiwan, Republic of China.

ABBREVIATIONS: DPH, phenytoin; CBZ, carbamazepine; LTG, lamotrigine; EGTA, ethylene glycol bis(β-aminoethyl ether)-*N*,*N*,*N*′,*N*′-tetraacetic acid; HEPES, 4-(2-hydroxyethyl)-1-piperazineethanesulfonic acid.

channel? And if so, can we tell more about the location and organization of the receptor? Because the highly selective binding of these anticonvulsants to the inactivated state rather than the resting state is a consequence of channel gating, characterization of the binding site for the anticonvulsants would not only be of pharmacological and pharmaceutical interest but also shed light on the gating conformational changes of the Na^+ channel. In this study, I examine the inhibition of Na^+ current by mixtures of different anticonvulsants and demonstrate that the Na^+ channel cannot be doubly occupied by DPH, CBZ, or LTG. It also is found that DPH, CBZ, and LTG are effective Na^+ channel inhibitors when applied externally, yet they are of no discernible effect when applied to the cytoplasmic side. Altogether these findings suggest that DPH, CBZ, and LTG bind to a common binding site located on the external side of neuronal Na^+ channels.

Materials and Methods

Cell preparation. Coronal slices of the brain were prepared from 7–14-day-old Long-Evans rats. The CA1 region was dissected from the slices and cut into small chunks. After treatment for 5–10 min at 37° in dissociation medium (82 mM Na_2SO_4, 30 mM K_2SO_4, 3 mM $MgCl_2$, 5 mM HEPES, and 0.001% phenol red indicator, pH 7.4) containing 0.5 mg/ml trypsin (Type XI; Sigma Chemical, St. Louis, MO), tissue chunks were moved to dissociation medium containing no trypsin but 1 mg/ml bovine serum albumin (Sigma) and 1 mg/ml trypsin inhibitor (Type II-S, Sigma). Each time when cells were needed, two or three chunks were picked and triturated to release single neurons.

Whole-cell recording. The dissociated neurons were put in a recording chamber containing Tyrode's solution (150 mM NaCl, 4 mM KCl, 2 mM $MgCl_2$, 2 mM $CaCl_2$, and 10 mM HEPES, pH 7.4). Whole-cell voltage clamp recordings were obtained using pipettes pulled from borosilicate micropipettes (o.d., 1.55–1.60 mm; Hilgenberg, Malsfeld, Germany), fire polished, and coated with Sylgard (Dow-Corning, Midland, MI). Except for the internal anticonvulsant experiments (see Fig. 8), the pipettes were filled with the standard internal solution containing 75 mM CsCl, 75 mM CsF, 2.5 mM $MgCl_2$, 5 mM HEPES, and 5 mM EGTA, pH adjusted to 7.4 by CsOH. For the experiments studying the effect of internal anticonvulsants, 300 μM LTG, 300 μM CBZ, or 100 μM DPH was added to the standard internal solution. Seal was formed, and the whole-cell configuration was obtained in Tyrode's solution. The cell then was lifted from the bottom of the chamber and moved in front of an array of flow pipes (microcapillary; Hilgenberg; content, 1 μl, length, 64 mm) emitting external recording solutions, which were Tyrode's solution with or without different concentrations of drugs. DPH, CBZ, and LTG were dissolved in dimethylsulfoxide to make a 100 mM stock solution, which then was diluted into Tyrode's solution to attain the final concentrations desired. The final concentration of dimethylsulfoxide ($\leq$0.3%) was not found to have significant effect on Na^+ currents. Currents were recorded at room temperature (~25°) with an Axoclamp 200A amplifier, filtered at 5 kHz with four-pole Bessel filter, digitized at 20–50-μsec intervals, and stored using a Digidata-1200 analog/digital interface along with the pCLAMP software (Axon Instruments, Foster City, CA). Residual series resistance was generally smaller than 1 MΩ after partial compensation (typically >80%). DPH and CBZ were from Sigma, and LTG was a kind gift from Wellcome Foundation (Kent, England). All statistical values are given as mean ± standard deviation.

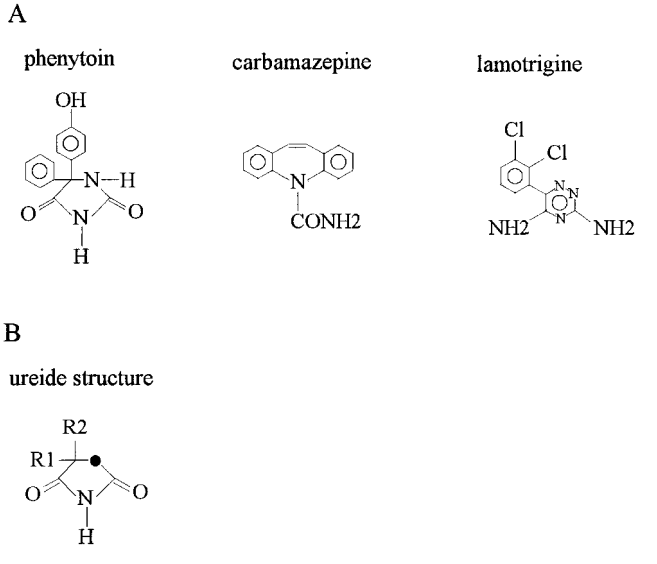

Fig. 1. Chemical structure of the drugs. A, Structures of phenytoin, carbamazepine, and lamotrigine. B, The ureide structure that could be found in many anticonvulsants, including phenytoin but not carbamazepine or lamotrigine. *Black dot*, substitutions in the ring, which could be —C—N—, —N—, —C—C—, —O—, or —C—. R1 and R2 are side chain groups attached to the five- or six-member ring.

Results

The shift of inactivation curve by 100 μM CBZ plus 100 μM LTG argues against simultaneous occupancy of the channel by CBZ and LTG. It has been shown that steady state inactivation curve of Na^+ channels is shifted by DPH, CBZ, and LTG (Matsuki *et al.*, 1984; Willow *et al.*, 1985; Lang *et al.*, 1993; Kuo and Bean, 1994a; Xie *et al.*, 1995; Kuo and Lu, 1997; Kuo *et al.*, 1997). The shift is well explained by a scheme that the anticonvulsants bind to the inactivated channels with a much higher affinity than to the resting channels (Fig. 2A). According to this scheme, in the control condition the fraction of channels in state R at different membrane potentials (V) can be approximated by a Boltzmann distribution: $1/(1 + \exp[(V - V_h)/k]$ (the "inactivation curve"). In the presence of an anticonvulsant, the shape of the inactivation curve (the slope factor k) remains the same, but the midpoint of the curve (V_h) would be shifted by ΔV, which is given by the following equation (Bean *et al.*, 1983; Kuo and Bean, 1994a):

$$exp(\Delta V/k) = [1 + (D/K_I)]/[1 + (D/K_R)] \quad (1)$$

where D is the concentration of the anticonvulsant, and K_R and K_I are the dissociation constants for the resting and inactivated states, respectively. Because K_R is generally in the millimolar range for these anticonvulsants in rat hippocampal neurons (Kuo and Bean, 1994a; Kuo and Lu, 1997; Kuo *et al.*, 1997), item D/K_R is small with ~100 μM anticonvulsant. The interaction between anticonvulsants and the resting channels thus is disregarded for a more straightforward (but still valid) conceptualization of the ΔV in the presence of multiple drugs. Deletion of D/K_R becomes

$$exp(\Delta V/k) \cong 1 + (D/K_I) \quad (2)$$

Based on rationales of eqs. 1 and 2, one may derive the ΔV in the presence of two different anticonvulsants. If the two drugs have the same binding site in the channel, then the binding of one drug to the inactivated channel would pre-

clude the binding of the other drug (the one-site model; Fig. 2B), and ΔV is given by

$$exp(\Delta V/k) \cong 1 + (D1/K_{I,1}) + (D2/K_{I,2}) \quad (3)$$

where D1 and D2 are the concentrations of the two drugs, and $K_{I,1}$ and $K_{I,2}$ are the K_I values for drug 1 and drug 2, respectively. However, if the inactivated channel can be doubly occupied by the drugs (i.e., there are different binding sites for different drugs), then there would be occupancy of a new state (ID_1D_2), the inactivated Na^+ channel simultaneously occupied by two different drugs (the two-site model, Fig. 2C), and the shift of inactivation curve is given by

$$exp(\Delta V/k) \cong 1 + (D1/K_{I,1}) + (D2/K_{I,2}) + (D1/K_{I,1}) \times (D2/K_{I,2}) \quad (4)$$

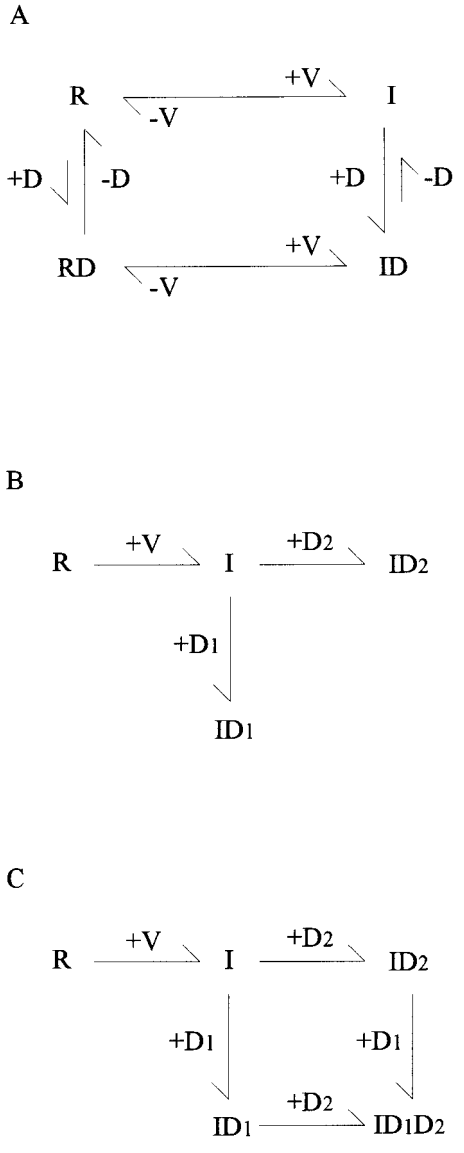

Fig. 2. Simplified gating schemes illustrating possible actions of the anticonvulsants phenytoin, carbamazepine, and lamotrigine. A, *R and I*, Resting and inactivated states of the Na^+ channel, respectively. *D*, Anticonvulsant drugs. *RD and ID*, anticonvulsant drug-bound resting and inactivated states, respectively. The anticonvulsant drugs have much higher affinity to the I state than to the R state. Thus, the +D arrow (drug binding rates) between I and ID is much larger than the −D arrow (drug unbinding rates), but the relative size of the arrows between R and RD is just the opposite. Membrane depolarization (+V) tends to move the channel from the resting to the inactivated state, whereas membrane hyperpolarization (−V) has the opposite effect. B, During depolarization, most channels are moved to the inactivated state. If anticonvulsants drug 1 and drug 2 (D1 and D2) share the same receptor in the inactivated channel, then the channel can be bound by either D1 or D2 but not both, even when saturating concentrations of D1 and D2 are present. C, If different anticonvulsants have separate receptors, then the inactivated Na^+ channels may be doubly occupied by both D1 and D2, especially when saturating concentrations of D1 and D2 are present.

The shift of inactivation curve predicted by eq. 3 is obviously different from that predicted by eq. 4. One may use saturating concentrations of the drugs to make the difference large and easily discernible. Fig. 3, A–C, shows the shift of inactivation curve (ΔV) in high concentrations of CBZ and LTG. The ΔV documented in these neurons in the presence of CBZ or LTG alone is consistent with previous observations (Kuo and Lu, 1997; Kuo *et al.*, 1997), where the shift of inactivation curve over a wide range of drug concentration yielded a K_I value of ~25 μM for CBZ and a K_I value of ~9 μM for LTG. Based on these K_I values and a slope factor $k = 6$, the ΔV in the presence of 100 μM CBZ plus 100 μM LTG would be 16.7 mV by eq. 3 and 24.6 mV by eq. 4. The experimental data (~16.6 mV, Fig. 3C) is much closer to the former than to the latter. Also, the inactivation curve in 100 μM CBZ plus 100 μM LTG typically lies between that in 200 μM CBZ and that in 200 μM LTG, rather than being far more negative to that in 200 μM LTG (Fig. 3, B and C). These findings argue against significant existence of the doubly occupied state ID_1D_2. In other words, it seems that the Na^+ channel cannot be occupied simultaneously by CBZ and LTG.

The shift of inactivation curve by 100 μM DPH plus 100 μM CBZ plus 100 μM LTG suggests no double occupancy of the channel by any two drugs. Fig. 4A summarizes the ΔV in high concentrations of DPH and LTG. The ΔV in 200 μM DPH is not available because of the low solubility of DPH in Tyrode's solution (~100 μM, pH 7.4, 25°). The ΔV in the presence 100 μM DPH also is consistent with previous observations in the same system (Kuo *et al.*, 1997), where a K_I value for DPH of ~9 μM is documented. The experimental data of ΔV are 16.1 mV in 100 μM DPH plus 100 μM CBZ and 17.8 mV in 100 μM DPH plus 100 μM LTG. These values again are much closer to the predictions by eq. 3 (16.7 and 18.9 mV, respectively) than to the predictions by eq. 4 (24.6 and 29.9 mV, respectively). Moreover, the ΔV in the presence of 100 μM DPH plus 100 μM CBZ plus 100 μM LTG is 18.5 mV (Fig. 4, B and C). This is slightly smaller than the ΔV value in 300 μM LTG (19.1 mV) and is close to the predicted value according to the equation (19.8 mV, calculated using aforementioned K_I values of DPH, CBZ, and LTG, and a slope factor $k = 6$):

$$exp(\Delta V/k) \cong 1 + (D1/K_{I,1}) + (D2/K_{I,2}) + (D3/K_{I,3}) \quad (5)$$

where D1, D2, and D3 are the concentrations of the three drugs, and $K_{I,1}$, $K_{I,2}$, and $K_{I,3}$ are the K_I values for drugs 1, 2, and 3, respectively. Eq. 5 is an extension of eq. 3. On the other hand, if the three drugs can all bind to the channel simultaneously, then an extension of eq. 4 based on incorporation of the triply occupied state $ID_1D_2D_3$ and three doubly occupied states would predict a much larger ΔV value (39.6 mV) by 100 μM DPH plus 100 μM CBZ plus 100 μM LTG. These findings suggest that one inactivated channel can be

occupied by only one drug molecule, even though high concentrations of DPH, CBZ, and LTG are present.

The recovery kinetics of the inhibited Na^+ current are similar in different drug concentrations. In addition to the effect on the steady state inactivation curve, one may examine the existence of doubly occupied inactivated channels from a kinetic point of view. Fig. 5, A–D, shows the time course of recovery of Na^+ current from inhibition by either CBZ or LTG. Here, 100 and 200 μM drug concentrations (quite higher than the apparent K_I value for each drug) are

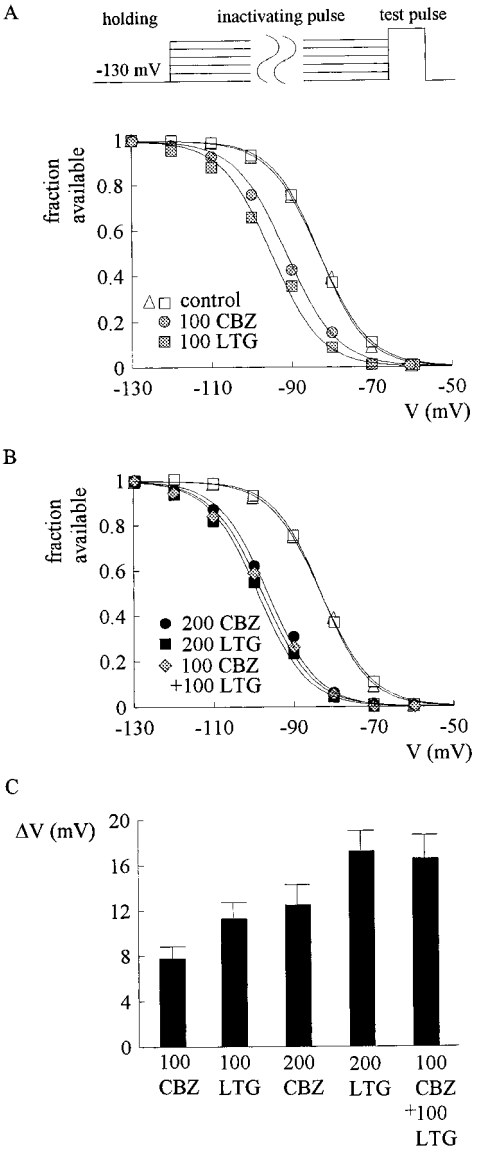

Fig. 3. Shift of the inactivation curve by CBZ and LTG. A, and B, The cell was held at −130 mV and stepped every 15 sec to the inactivating pulse (−130 to −60 mV) for 9 sec. The channels that remain available after each inactivating pulse were assessed by the peak currents during a following short test pulse to 0 mV for 5 msec. The fraction available is defined as the normalized peak current (relative to the current evoked with an inactivating pulse at −130 mV) and is plotted against the voltage of the inactivating pulse (V). Both parts A and B contain the same two sets of control data, which were obtained before and after the five sets of data in the presence of drugs to demonstrate the lack of significant voltage drift during this long experiment. The lines are fits with a Boltzmann function $1/(1 + \exp[(V - V_h)/k)]$, with V_h values (in mV) of −83.1, −83.1, −91.3, −95.1, −96.4, −98.1, and −97.7, and k values of 6.2, 5.9, 6.3, 6.2, 5.8, 6.1, and 6.1 for control (before drugs), control (after drugs), 100 μM CBZ, 100 μM LTG, 200 μM CBZ, 200 μM LTG, and 100 μM CBZ plus 100 μM LTG, respectively. C, Shift of the inactivation curve by CBZ and/or LTG. The shift (ΔV) is determined in each cell by the difference between V_h in control and in the presence of anticonvulsant drugs. The values of ΔV (in mV) are 7.8 ± 1.1, 11.3 ± 1.4, 12.5 ± 1.8, 17.2 ± 1.8, and 16.6 ± 2.1 (all from five sets) for 100 μM CBZ, 100 μM LTG, 200 μM CBZ, 200 μM LTG, and 100 μM CBZ plus 100 μM LTG, respectively.

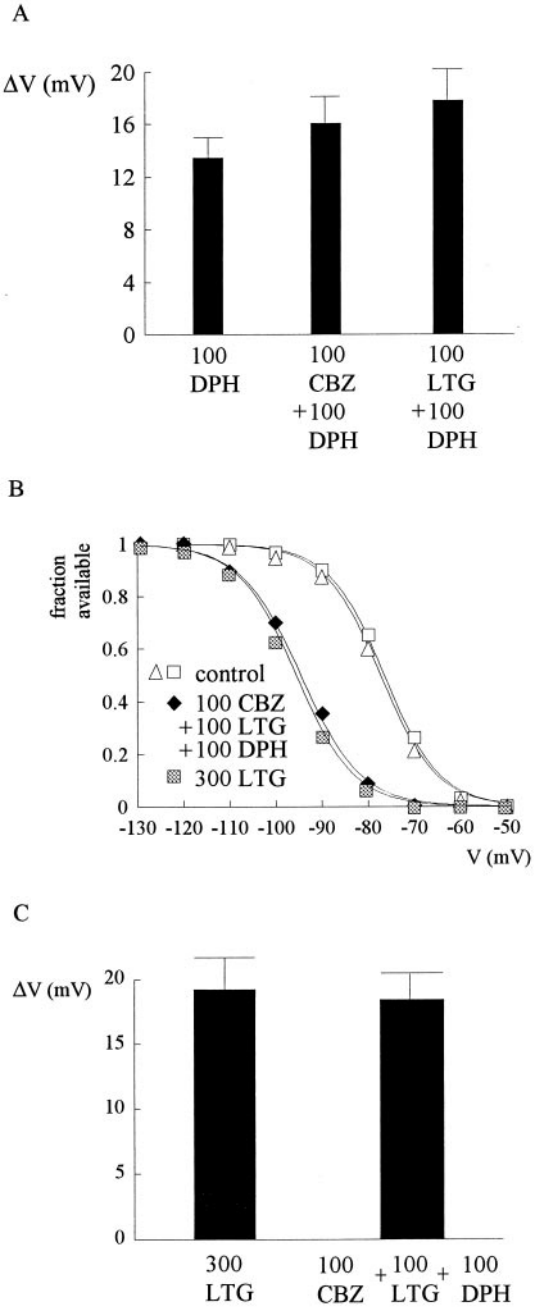

Fig. 4. Experiments similar to those in Fig. 3 to demonstrate shift of the inactivation curve (ΔV) by different combinations of anticonvulsants DPH, CBZ, and LTG. A, The values of ΔV (in mV) are 13.4 ± 1.6, 16.1 ± 2.0, and 17.8 ± 2.3 (all from five sets) for 100 μM DPH, 100 μM CBZ plus 100 μM DPH, and 100 μM LTG plus 100 μM DPH, respectively. B, and C, The inactivation curves in 300 μM LTG and in 100 μM CBZ plus 100 μM LTG plus 100 μM DPH. The lines are fits with a Boltzmann function $1/(1 + \exp[(V - V_h)/k)]$, with V_h values (in mV) of −77.3, −76.6, −95.4, and −94.8 and k values of 5.9, 6.0, 6.3, and 6.1 for control (before drugs), control (after drugs), 300 μM LTG, and 100 μM CBZ plus 100 μM LTG plus 100 μM DPH, respectively. The values of ΔV (in mV) are 19.2 ± 2.5 and 18.5 ± 1.9 (both from eight data sets) for 300 μM LTG and 100 μM CBZ plus 100 μM LTG plus 100 μM DPH, respectively.

used to ensure that a major portion of the inactivated channels is bound by the anticonvulsant at the end of the long inactivating prepulse. In the control (drug-free) condition, a major part (~70%) of the Na^+ current recovers within 10 msec at −120 mV after the long inactivating pulse (Fig. 5, A–D). When the anticonvulsant is present, there is a small but very fast component of recovery in the first 10 msec. This component presumably represents the recovery from residual drug-free inactivated Na^+ channels in the presence of CBZ or LTG and therefore is smaller in higher drug concentrations. On the other hand, the majority of the recovery after 10 msec should be from the drug-bound channels. The recovery courses after 10 msec are quite similar in different drug concentrations, which could be demonstrated by the time constants of the forced monoexponential fits to this part of the recovery courses. This is consistent with the notion that

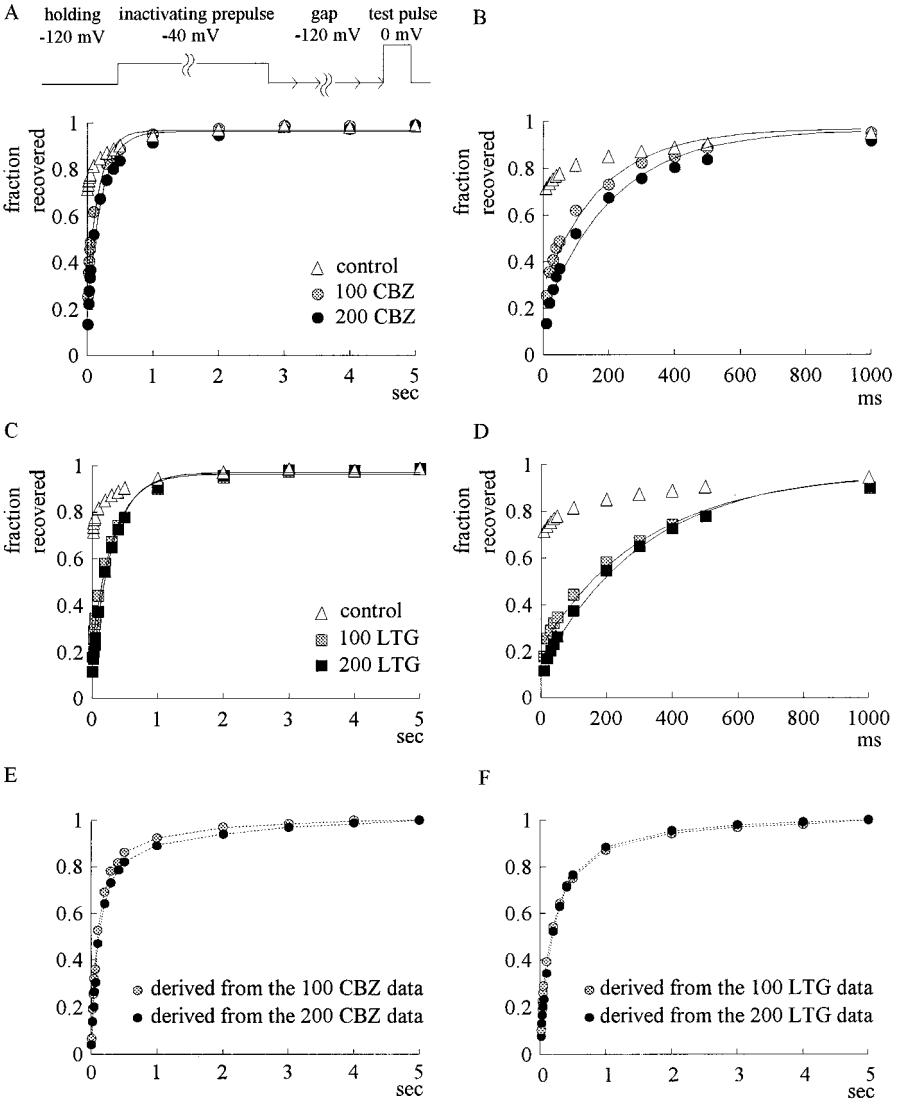

Fig. 5. Recovery from inhibition by CBZ or LTG. A, In control or in the continuous presence of 100 or 200 μM CBZ, the cell was held at −120 mV and then prepulsed to −40 mV for 9 sec to reach a maximal (steady state) block of Na^+ current by CBZ. The cell then was stepped back to a recovery gap potential at −120 mV for variable length before being stepped again to a short test pulse at 0 mV for 5 msec to assess the available current. The pulse protocol was repeated every 15 sec. After long recovery period (~5 sec), the peak currents at the test pulse reached a "steady state" level, which was slightly reduced in CBZ than in control because of the very mild inhibition of resting channels by high concentrations of CBZ. The fraction recovered is defined as the normalized peak current at the test pulse (relative to the peak current at the test pulse after a 5-sec recovery gap period) and is plotted against the length of the recovery gap period. *Lines*, monoexponential fits to the recovery course after 10 msec in drugs and are of the form: fraction recovered = $0.97 - 0.64\exp[-(t - 10)/180)]$ for 100 μM CBZ (t denotes length of the recovery gap potential in msec), and fraction recovered = $0.96 - 0.75\exp[(-(t - 10)/197)]$ for 200 μM CBZ. B, The first 1 sec of the recovery courses in part A is replotted with a different time scale for a better illustration of the data. The lines are the same as those in part A. C, Similar experiments to those in part A were repeated in the same cell to demonstrate the recovery kinetics in 100 and 200 μM LTG. *Lines*, monoexponential fits for the recovery course after 10 msec and are of the form: fraction recovered = $0.97 - 0.73\exp[(-(t - 10)/325)]$ for 100 μM LTG, and fraction recovered = $0.97 - 0.82\exp[(-(t - 10)/317)]$ for 200 μM LTG. D, The first 1 sec of the recovery courses in part C are replotted with a different time scale for a better illustration of the data. *Lines*, same as those in part C. E, The recovery courses in part A are not purely from the CBZ-bound channels but are "contaminated" by the small amount of drug-free channels. The "contamination" is corrected (for details, please refer to the text) to yield the recovery courses of the CBZ-bound channels in this plot. *Dashed lines*, connecting the data points and have no mathematical meanings. Note that the recovery courses are very similar to each other whether it is derived from the 100 μM or 200 μM CBZ data in part A. F, Similar treatment of the data in part C yields the recovery courses of the LTG-bound channels. *Dashed lines*, connecting the data points and have no mathematical meanings. Note again that the courses derived from the 100 or 200 μM LTG data in part C are quite similar to each other.

these anticonvulsants interact with Na^+ channels via a simple bimolecular reaction, where the drug unbinding rate should be unrelated to ambient drug concentrations.

Fig. 5, E and F, demonstrates another quantitative analysis of the recovery courses in different concentrations of CBZ and LTG. Given a simple bimolecular reaction and a K_I value of ~25 μM for CBZ, at the end of the long inactivating pulse the proportions of drug-free Na^+ channels would be 1/(1 + 4) and 1/(1 + 8) for 100 and 200 μM CBZ, respectively (100/25 = 4, 200/25 = 8, assuming steady state effect). To correct for the "contamination" from the recovery of the drug-free channel, 1/5 is subtracted from every data point in 100 μM CBZ and 1/9 is subtracted from every data point in 200 μM CBZ in Fig. 5A. The two sets of corrected data points then are normalized to the last point (the point at 5-sec recovery period) in each set to yield the recovery courses of the CBZ-bound channel in Fig. 5E. The recovery courses of the LTG-bound channel in Fig. 5F are obtained by similar treatment of the data points in Fig. 5C (using a K_I value of ~9 μM for LTG). In Fig. 5, E and F, the recovery kinetics of the drug-bound channel are very similar in different concentrations of each drug. However, a comparison between Fig. 5E and Fig. 5F reveals faster recovery from CBZ-bound channels than from LTG-bound channels, suggesting slower unbinding rate of LTG from the channel.

Recovery of the inhibited Na^+ currents in 100 μM CBZ plus 100 μM LTG is faster than that in 100 μM LTG alone. Fig. 6, A–D, examines the recovery kinetics in 100 μM CBZ plus 100 μM LTG. If the channel can be doubly occupied by CBZ and LTG, then the recovery from inhibition by 100 μM CBZ plus 100 μM LTG is expected to be slower than those in 100 μM CBZ or in 100 μM LTG. This is because in the presence of saturating concentrations of both drugs, most channels would be in the double-occupancy state (state ID_1D_2 in Fig. 2C) if there are separate drug binding sites. Recovery from state ID_1D_2 conceivably would be slower than that from ID_1 or ID_2 because it is one step farther from the R state. Fig. 6, A and B, however, shows that the recovery course in 100 μM CBZ plus 100 μM LTG is not slower but is even faster than the recovery in 100 μM LTG. Although drug-free inactivated channels must be less prevalent in 100 μM CBZ plus 100 μM LTG than in 100 μM LTG at the end of the long inactivating prepulse, the absolute value of fraction recovered is higher in 100 μM CBZ plus 100 μM LTG than in 100 μM LTG at almost every time point. In all four cells examined, the half-recovery time is always shorter, or at least not longer, in 100 μM CBZ plus 100 μM LTG than in 100 μM LTG alone (Fig. 6C). The faster recovery in the presence of 100 μM CBZ plus 100 μM LTG strongly suggests that the binding of one drug (e.g., the faster unbinding drug CBZ) decreases the binding of the other (e.g., the slower unbinding drug LTG). This is consistent with the foregoing argument that CBZ binding and LTG binding to the channel are mutually exclusive.

Fig. 6D demonstrates another analysis of the recovery course in 100 μM CBZ plus 100 μM. If there is a common receptor for CBZ and LTG, then the proportion of CBZ-bound channel at the end of the inactivating pulse (assuming steady state effect is reached) is 4/(1 + 4 + 11.1) or 4/16.1 (100/25 = 4, 100/9 = 11.1), and the proportions of LTG-bound and drug-free channels are 11.1/16.1 and 1/16.1, respectively. On the other hand, if there are separate and independent binding sites for CBZ and LTG, then the proportions of different drug-bound states should be given by (the chance of a drug-free CBZ site plus the chance of an occupied CBZ site) multiplied by (the chance of a drug-free LTG site plus the chance of an occupied LTG site) or (1/5 + 4/5) × (1/12.1 + 11.1/12.1),

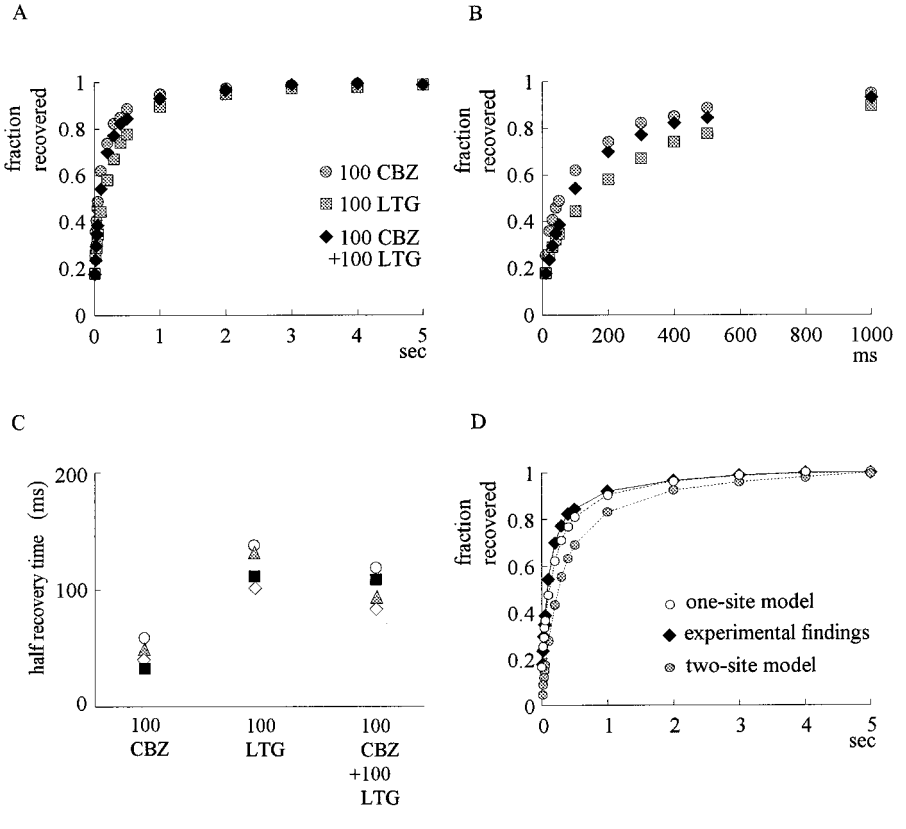

Fig. 6. Recovery from inhibition by 100 μM CBZ plus 100 μM LTG. A, Recovery from inhibition by 100 μM CBZ plus 100 μM LTG were documented in the same cell as that in Fig. 5. The experimental protocol is also the same as that in Fig. 5A. The recovery courses in 100 μM CBZ and 100 μM LTG are taken from Fig. 5, A and C, and are replotted here for comparison. B, The first 1 sec of the recovery courses in part A is replotted with a different time scale. Note the faster recovery course in 100 μM CBZ plus 100 μM LTG than in 100 μM LTG. C, Because the recovery courses in 100 μM CBZ plus 100 μM LTG cannot be reasonably approximated by monoexponential functions, the half recovery time is used as a simple parameter to compare the recovery kinetics in different conditions. The half recovery time is defined as the length of the recovery gap potential to recover half the current (fraction recovered equals 0.5). The same symbols represent data from the same cell. In every cell tested, the half recovery time is shorter in 100 μM CBZ plus 100 μM LTG than in 100 LTG alone. D, Based on rationales of a bimolecular reaction and the data in Fig. 5, E and F, the "theoretical" recovery courses in 100 μM CBZ plus 100 μM LTG are calculated according to the one-site model and the two-site model (for details, refer to the text). The lines are connecting the data points and have no mathematical meanings. The experimental findings (the same data as those in part A) are closer to the course predicted by the one-site model than to the course predicted by the two-site model.

which yields 1/60.5, 4/60.5, 11.1/60.5, and 44.4/60.5 for drug-free, CBZ-bound (but not LTG-bound), LTG-bound (but not CBZ-bound), and CBZ and LTG doubly bound channels, respectively. We have noted the recovery time courses of CBZ-bound channels and LTG-bound channels in this cell in Fig. 5, E and F. If D1 and D2 bind to different binding sites and the unbinding processes of each drug are unrelated events, then the recovery from ID_1D_2 would mean the probability of unbinding of both bound drugs, which should be equal to the probability of CBZ unbinding multiplied by the probability of LTG unbinding. Thus, the recovery course of CBZ and LTG doubly bound channels (state ID_1D_2 in Fig. 2C), if they do exist, should be the product of the recovery course of CBZ-bound channel (Fig. 5E) and the recovery course of LTG-bound channel (Fig. 5F). The recovery courses in 100 μM CBZ plus 100 μM LTG predicted by the one-site model and the two-site model thus are given by the next equations.

If there is only a common binding site for CBZ and LTG (the one-site model), then

$$\text{Recovery course} = 1/16 + (4/16.1) \times C + (11.1/16.1) \times L \quad (6)$$

If there are separate binding sites for CBZ and LTG (the two-site model), then

$$\text{Recovery course} = 1/60.5 + (4/60.5) \times C + (11.1/60.5) \times L + (44.1/60.5) \times C \times L \quad (7)$$

where C stands for the recovery courses of the CBZ-bound channels in Fig. 5E (the one derived from 100 μM CBZ is used), and L stands for the recovery courses of the LTG-bound channels in Fig. 5F (the one derived from 100 μM LTG is used). The calculated results are plotted in Fig. 6D. It is evident that the experimental data are well predicted by the one-site model but not by the two-site model. This finding further strengthens the argument that CBZ and LTG share a common binding site in the inactivated Na^+ channels.

Recovery of the inhibited Na^+ currents in 100 μM CBZ plus 100 μM DPH also is no slower than that in 100 μM DPH alone. Fig. 7, A–D, demonstrates the recovery course in 100 μM CBZ plus 100 μM DPH. The findings are very similar to those in Fig. 6, A–D. Fig. 7, A and B, shows the recovery courses in 100 μM CBZ, 100 μM DPH, and 100 μM CBZ plus 100 μM DPH. The recovery in 100 μM CBZ plus 100 μM DPH is not slower than the recovery in 100 μM DPH (although the drug-free inactivated channels must be less prevalent in 100 μM CBZ plus 100 μM DPH than in 100 μM DPH at the end of the long prepulse). The half recovery time is also shorter, or at least not longer, in 100 μM CBZ plus 100 μM DPH than in 100 μM DPH (Fig. 7C). Based on the same rationales underlying Figs. 5, E and F, and 6D, and a K_I value of ~25 μM for CBZ as well as a K_I value of ~9 μM for DPH, the recovery courses in 100 μM CBZ plus 100 μM DPH predicted by the one- and two-site models are derived from the data in Fig. 7A and are plotted in Fig. 7D. The observed recovery course in 100 μM CBZ plus 100 μM DPH again is well predicted by the one-site model. Altogether, the kinetic data in Figs. 6 and 7 strongly argue against the existence of channels doubly occupied by saturating concentrations of CBZ, LTG, or DPH and are thus suggestive of a common binding site for these anticonvulsants in inactivated Na^+ channels.

DPH, CBZ, and LTG have no significant effect on the Na^+ current if applied internally. In previous experiments, DPH, CBZ, and LTG are applied externally (applied to the extracellular side). However, the uncharged form of these anticonvulsants cross the membrane easily. Because

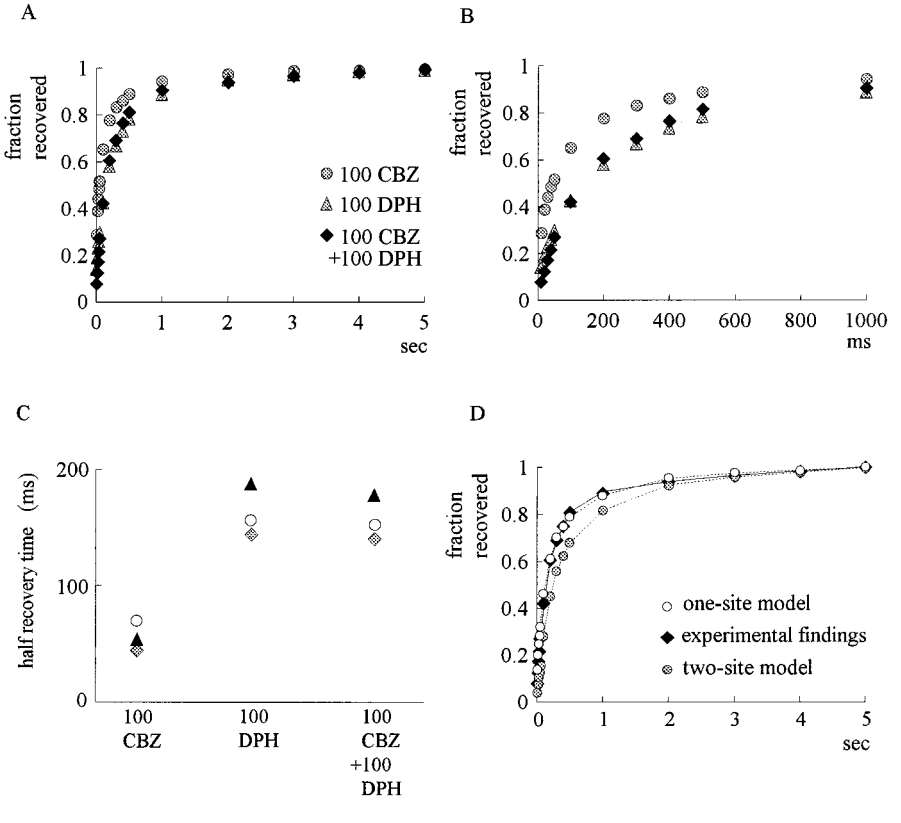

Fig. 7. Recovery from inhibition by 100 μM CBZ plus 100 μM DPH. A, Recovery from inhibition by 100 μM CBZ, 100 μM DPH, and 100 μM CBZ plus 100 μM DPH were examined by the same protocol as that in Fig. 5A. B, The first 1 sec of the courses in part A are replotted with a different time scale. Note that the recovery in 100 μM CBZ plus 100 μM DPH is not slower than the recovery in 100 μM DPH alone. C, In every cell tested, the half recovery time (defined in the legend of Fig. 6C) is not longer in 100 μM CBZ plus 100 μM DPH than in 100 μM DPH alone. The same symbols represent data from the same cell. D, The recovery courses in 100 μM CBZ plus 100 μM DPH predicted by the one-site model and the two-site model are derived based on the same rationales underlying those in Figs. 5, E and F, and 6D. The lines are connecting the data points and have no mathematical meanings. The experimental findings (the same data as those in part A) again are closer to the course predicted by the one-site model than to the course predicted by the two-site model.

there is no rapid "wash" of the intracellular space, the intracellular drug concentration may be similar to the external drug concentration in those experiments. Thus one cannot tell whether the anticonvulsants inhibit Na^+ channels from outside or inside based on the previous experiments. Taking advantage of the rapid and continuous solution change of the extracellular space in the experimental system, I examined the effect of internal LTG by adding 300 μM LTG to the pipette solution. Now, the LTG crossing the membrane and reaching the outside is quickly washed away. Thus, there will be no significant build-up of LTG concentrations in the external solution. In ~10 min after breakthrough into the cell, when the intracellular space should be completely dialyzed by the LTG-containing internal solution, Na^+ current is still elicitable by a test pulse from a holding potential of −65 mV, and the current amplitude is ~10% of that elicited from a holding potential of −120 mV (Fig. 8A). This is similar to the case with drug-free internal solution and is very different from the effect of 300 μM external LTG (see the inactivation curves in Fig. 4). Moreover, with 300 μM internal LTG and a holding potential of −65 mV, the elicited Na^+ current still is significantly inhibited by 30 μM external LTG, further supporting that the "control" current in Fig. 8A is not a residual current already under significant inhibition by 300 μM LTG.

To elucidate this point more quantitatively, the inactivation curves in the absence and presence of 30 μM external LTG are obtained with 300 μM LTG in the intracellular space. The shift of inactivation curve (ΔV) by 30 μM external LTG in the presence of 300 μM internal LTG is very similar to the ΔV by 30 μM external LTG with drug-free internal solution (Fig. 8B). In contrast, if the Na^+ current is already under significant inhibition by 300 μM LTG, there should be only negligible effect by the addition of 30 μM LTG ($\Delta V < 0.6$ mV by eq. 2). Significant effects of 30 μM external DPH and 30 μM external CBZ also are observed with 100 μM internal DPH and 300 μM internal CBZ, respectively (Fig. 8, C and D). Thus, internal DPH, CBZ, and LTG all seem to show no significant effect on the Na^+ current, which implies an external rather than an internal location of the binding site for these anticonvulsants in the Na^+ channel.

Discussion

DPH, CBZ, and LTG have qualitatively very similar inhibitory effects on central neuronal Na^+ currents. Based on the steady state and kinetic data in this study, I propose that such similar effects arise, at least in part, from a common

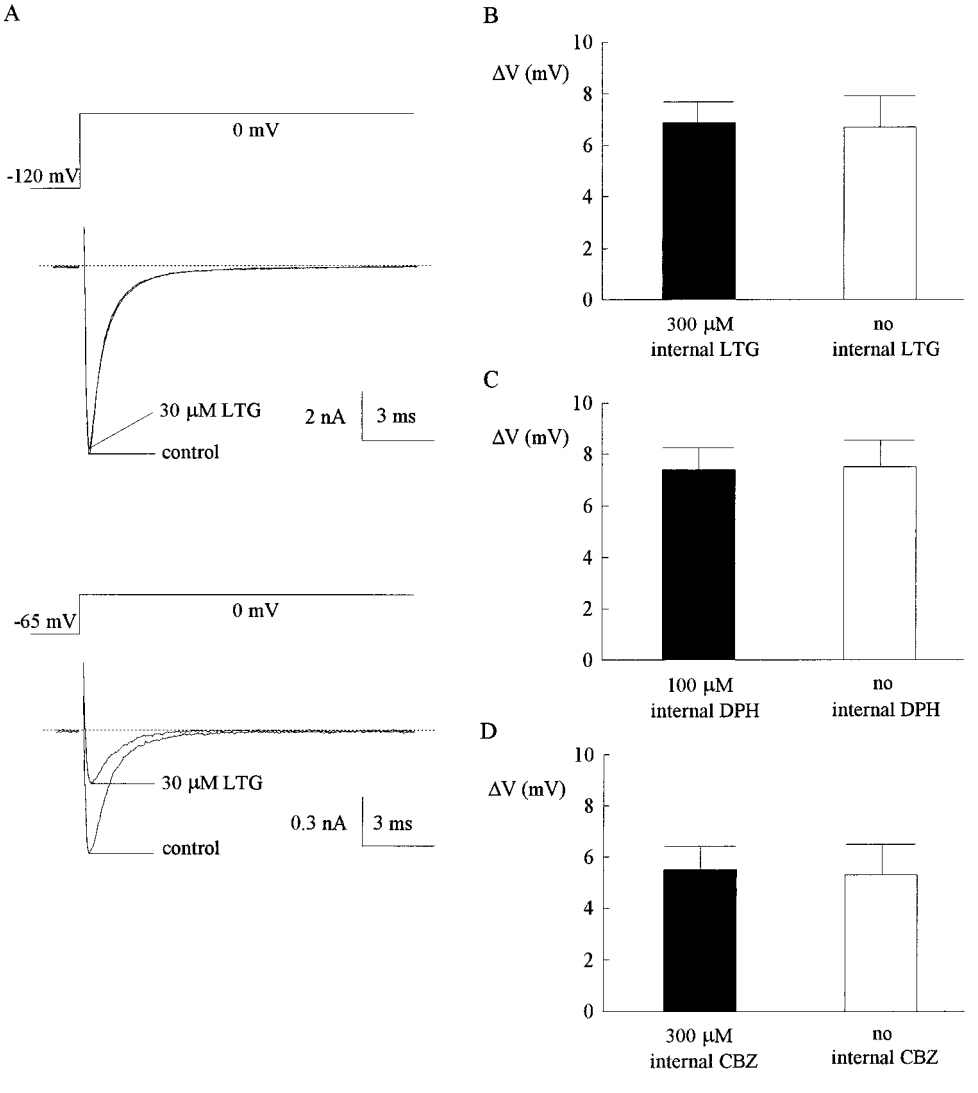

Fig. 8. Internal LTG, DPH, or CBZ has no effect on Na^+ currents. A, Sample Na^+ currents in a cell in which the pipette contained standard internal solution plus 300 μM LTG. After the whole-cell configuration was obtained, the Na^+ current was elicited by a short step depolarization to 0 mV for 15 msec from holding potentials −120 mV or −65 mV (the "control" sweeps in both panels). For the next 10 min, the current had shown no significant change. The cell then was moved into external solution containing 30 μM LTG, which significantly inhibits the Na^+ current elicited from a holding potential of −65 mV. B, The shift of inactivation curve (ΔV) by 30 μM external LTG in five cells containing 300 μM internal LTG is 6.9 ± 0.8 mV (■, determined by the same procedures as those in Fig. 3). As a comparison, the ΔV by 30 μM external LTG in five cells containing no internal anticonvulsants is 6.7 ± 1.2 mV (□). C, Similar experiments as those in part B. The ΔV by 30 μM external DPH in five cells containing 100 μM internal DPH is 7.4 ± 0.8 mV (■), and the ΔV by 30 μM external DPH in five cells containing no internal anticonvulsants is 7.5 ± 1.0 mV (□). D, Similar experiments as those in part B. The ΔV by 30 μM external CBZ in five cells containing 300 μM internal CBZ is 5.5 ± 0.9 mV (■), and the ΔV by 30 μM external CBZ in five cells containing no internal anticonvulsants is 5.3 ± 1.2 mV (□).

anticonvulsant binding site located on the external side of neuronal Na^+ channels.

No double occupancy of the Na^+ channel by anticonvulsants DPH, CBZ, or LTG. DPH, CBZ, and LTG all preferentially bind to the fast inactivated state rather than to the resting state of Na^+ channels (Matsuki *et al*., 1984; Willow *et al*., 1985; Lang *et al*., 1993; Kuo and Bean, 1994a; Xie *et al*., 1995; Kuo and Lu, 1997; Kuo *et al*., 1997), and the interaction between these anticonvulsants and the inactivated Na^+ channel is a bimolecular reaction (one-to-one binding process; Kuo and Bean, 1994a; Kuo and Lu, 1997; Kuo *et al*., 1997). In this study, it is shown that the rule of "single occupancy" is still observed when two or more anticonvulsants are simultaneously present in the system. The shift of inactivation curve is quantitatively incompatible with a model that the channel can be simultaneously occupied by two different drug molecules yet is well in line with a scheme that the binding of one drug precludes the binding of the others. The faster recovery from inhibition by a mixture of a fast-unbinding drug (e.g., CBZ) and a slow-unbinding drug (e.g., LTG) than from the inhibition by one single slow-unbinding drug further strengthens the mutual exclusiveness among DPH, CBZ, and LTG binding to the Na^+ channel.

A common receptor for DPH, CBZ, and LTG versus an allosteric interaction among the drugs. The mutual exclusiveness among the binding of different drugs to a channel may result from either an allosteric mechanism or a direct competition mechanism. The direct competition mechanism assumes that different drugs bind to the same receptor site. The allosteric mechanism assumes that different drugs bind to different receptors in the channel, but these different receptors do not coexist in one channel conformation. The scheme in Fig. 2B depicts only one inactivated state, which is connotative of a direct competition mechanism. For the allosteric model, the I state in Fig. 2B should be subdivided into at least three different inactivated states, I′, I″, and I‴, which have the receptor for DPH, CBZ, and LTG, respectively. Binding of DPH to I′, for example, would stabilize the channel to state I′ and thus prevent the binding of CBZ and LTG.

If the rate constants between the different inactivated states in an allosteric model are appropriately manipulated (e.g., assuming a rapid equilibrium among I′, I″, I‴, and so on), the steady state effect and the reaction kinetics in the presence of multiple drugs could be very similar to those obtained with a direct competition model. Thus, just based on findings in this study, it may be difficult to differentiate between the allosteric model and the direct competition model. However, a direct competition model is far simpler than a scheme containing multiple inactivated states, and most importantly, the existence of multiple inactivated states bearing different anticonvulsant receptors is not compatible with some characteristics previously described for the interaction between the anticonvulsants and the channel. For example, the affinity of DPH toward Na^+ channels at each holding potential is tightly correlated with channel inactivation, and the drug affinity curve (plotting affinity against membrane potential) is essentially a mirror image of the fast inactivation curve across the voltage axis [see Fig. 2 of Kuo and Bean (1994a); there also are similar patterns of affinity change for CBZ and LTG at different holding potentials (Kuo and Lu, 1997; Kuo *et al*., 1997)]. If there are three different fast inactivated states, each to be bound by only one anticonvulsant, then there would be a shift in the voltage axis of the two curves and the two curves can no longer be mirror image to each other. Given the simplest case that I′, I″, and I‴ each accounts for one third of total fast inactivation at equilibrium, the shift would be as large as ~6.6 mV (the natural logarithm of 1/3 times a slope factor 6), which should be easily discernible. I therefore conclude that DPH, CBZ, and LTG most likely bind to a common receptor in neuronal Na^+ channels.

Nature of the anticonvulsant receptor in Na^+ channels. In view of the apparent dissimilarity in chemical structure of DPH, CBZ, and LTG, it is interesting that these anticonvulsants would bind to a common receptor in Na^+ channels. DPH has two phenyl rings connected to a carbon atom in a ureide core. CBZ has two phenyl rings attached to another "bridge ring" to form a tricyclic structure. LTG is an even simpler compound and has just two phenyl rings connected to each other (Fig. 1A). Thus the only common structural motif shared by these three drugs is two phenyl groups separated by one to two C—C or C—N single bonds (1.5–3 Å). Such a motif presumably contains the major ligands interacting with the anticonvulsant receptor in Na^+ channels. It has been shown that the neutral, rather than charged, form of DPH is the active form inhibiting Na^+ currents (Morello *et al*., 1984). Thus, the binding between DPH and its receptor probably is nonionic. Other than ionic bond, drug/receptor interaction most likely involves hydrophobic bond (which represents a freeing of water molecules and a gain in entropy) or (induced) dipole-induced dipole bond [London forces or Debye forces; for review, see Zimmerman and Feldman (1989)]. The dissociation constants between these anticonvulsants and the inactivated channel are ~9–25 μM, which may be translated into a binding energy of 10.6–11.6 RT, or ~6.5 kcal/mol. Both the binding energy value and the notion that phenyl groups may be the major binding ligands are consistent with the proposal that the aforementioned nonionic bonds play a major role in the drug/receptor interaction under consideration here.

Because effective hydrophobic bonds or induced-dipole bonds require close proximity between the binding counterparts, the planar benzene ring would tend to form bond with the other planar benzene ring (Zimmerman and Feldman, 1989). I therefore propose that the common receptor for DPH, CBZ, and LTG in the inactivated Na^+ channel also contains two phenyl groups, which probably are part of the side chain groups of some aromatic amino acids constituting the channel. Each of the two phenyl group in the anticonvulsant thus would bind to a corresponding phenyl group in the receptor. It will be interesting to manipulate the benzene rings in the drugs by substitutions or changing their relative position to probe the drug/receptor interaction in more details. It also may be desirable to locate the presumable aromatic amino acids responsible for making of the anticonvulsant receptor. In this regard, it is interesting to note that mutation of an aromatic amino acid (phenylalanine) in the S6 segment of domain 4 of the Na^+ channel α subunits results in almost complete abolition of the use- and voltage-dependent block of local anesthetic etidocaine (Ragsdale *et al*., 1994).

Implications on the gating conformational changes of Na^+ channels. On depolarization, the Na^+ channel is activated quickly and then inactivated quickly because of

binding of an inactivating particle (the "ball and chain model"; Armstrong and Benzanilla, 1977; Armstrong, 1981) or a hinged peptide flap [the "hinged-lid model" (West, 1992)] to the internal pore mouth to block the pore. The open state is omitted in the schemes in Fig. 2 because the binding rates of DPH, CBZ, and LTG are so slow that no significant drug binding may happen to the very transient open state (Kuo and Bean, 1994a; Kuo and Lu, 1997; Kuo *et al*., 1997). Because the inactivated state may be considered as a state that is activated (open) but blocked at the internal pore mouth, the high affinity between anticonvulsants and the inactivated channel may arise from either channel activation or binding of the inactivating peptide (the hinged flap). In enzymatically treated channels that lack fast inactivation, DPH still shows significant inhibitory effect (Quandt, 1988). Quantitative comparison between the voltage dependence of the recovery from fast inactivation and the voltage dependence of the recovery from DPH inhibition also argues that DPH binding to the Na^+ channel does not require the presence of fast inactivation (Kuo and Bean, 1994b). Thus, the binding site for the anticonvulsants most likely is formed or is shaped into the "right" conformation during the activation processes of the channel [the "modulated receptor hypothesis" (Hille, 1977, 1993)]. Along with the findings that the anticonvulsant receptor is located on the extracellular side of the channel (Fig. 8), it seems that Na^+ channel activation involves multiple conformational changes not only in the pore (to become conducting of Na^+ ions) and on the cytoplasmic side (to bind the inactivating peptide or hinged flap) but also on the external side of the channel (to make the anticonvulsant receptor by realignment of side chains of some aromatic amino acids). The external conformational changes associated with channel gating also is supported by the previous finding that external application of some macromolecules impermeable to the membrane, such as antibodies against part of the primary sequence of Na^+ channel, shifts the steady state inactivation curve to more negative potentials (Meiri *et al*., 1987).

Acknowledgments

I thank the Wellcome Foundation Ltd. (Kent, England, and its branch in Taipei, Taiwan) for providing lamotrigine as a gift.

References

Armstrong CM (1981) Sodium channels and gating currents. *Physiol Rev* **61:**644–683.
Armstrong CM and Bezanilla F (1977) Inactivation of the sodium channel. II. Gating current experiments. *J Gen Physiol* **70:**567–590.
Bean BP, Cohen CJ, and Tsien RW (1983) Lidocaine block of cardiac sodium channels. *J Gen Physiol* **81:**613–642.
Brodie MJ, Richens A, Yuan AWC, and the UK Lamotrigine/Carbamazepine Monotherapy Trial Group (1995) Double-blind comparison of lamotrigine and carbamazepine in newly diagnosed epilepsy. *Lancet* **345:**476–479.
Hille B (1977) Local anesthetics: hydrophilic and hydrophobic pathways for the drug-receptor reaction. *J Gen Physiol* **69:**497–515.
Hille B (1993) *Ionic Channels of Excitable Membranes*, ed. 2., pp 408–412, Sinauer Associates, Sunderland, MA.
Kuo C-C and Bean BP (1994a) Slow binding of phenytoin to inactivated sodium channels in rat hippocampal neurons. *Mol Pharmacol* **46:**716–725.
Kuo C-C and Bean BP (1994b) Na^+ channels must deactivate to recover from inactivation. *Neuron* **12:**819–829.
Kuo C-C, Chen R-S, Lu L, and Chen RC (1997) Carbamazepine inhibition of neuronal Na^+ currents: quantitative distinction from phenytoin and possible therapeutic implications. *Mol Pharmacol* **51:**1077–1083.
Kuo C-C and Lu L (1997) Characterization of lamotrigine inhibition of Na+ channels in rat hippocampal neurons. *Br J Pharmacol* **121:**1231–1238.
Lang DE, Wang CM, and Cooper BR (1993) Lamotrigine, phenytoin and carbamazepine interactions on the sodium current present in N4TG1 mouse neuroblastoma cells. *J Pharmacol Exp Ther* **266:**829–835.
Lees G and Leach MJ (1993) Studies on the mechanism of action of the novel anticonvulsant lamotrigine (Lamictal) using primary neurological cultures from rat cortex. *Brain Res* **612:**190–199.
Matsuki N, Quandt FN, Ten Eick RE, and Yeh JZ (1984) Characterization of the block of sodium channels by phenytoin in mouse neuroblastoma cells. *J Pharmacol Exp Ther* **228:**523–530.
McLean MJ and McDonald RL (1983) Multiple actions of phenytoin on mouse spinal cord neurons in cell culture. *J Pharmacol Exp Ther* **227:**779–789.
McLean MJ and McDonald RL (1986) Carbamazepine and 10,11-epoxycarbamazepine produce use- and voltage-dependent limitation of rapidly firing action potentials of mouse central neurons in cell culture. *J Pharmacol Exp Ther* **238:**727–738.
Meiri H, Spira G, Sammar M, Namir M, Schwartz A, Komoriya A, Kosower EM, and Palti Y (1987) Mapping a region associated with Na channel inactivation using antibodies to a synthetic peptide corresponding to a part of the channel. *Proc Natl Acad Sci USA* **84:**5058–5062.
Miller AA, Wheatley P, Sawyer DA, Baxter MG, and Roth B (1986) Pharmacological studies on lamotrigine, a novel potential antiepileptic drug. I. Anticonvulsant profile in mice and rats. *Epilepsia* **27:**483–489.
Morello RS, Begenisich T, and Yeh JZ (1984) Determination of the active form of phenytoin. *J Pharmacol Exp Ther* **230:**156–161.
Quandt FN (1988) Modification of slow inactivation of single sodium channels by phenytoin in neuroblastoma cells. *Mol Pharmacol* **34:**557–565.
Ragsdale DS, McPhee JC, Scheuer T, and Catterall WA (1994) Molecular determinants of state-dependent block of Na^+ channels by local anesthetics. *Science* **265:**1724–1728.
Rogawski MA and Porter RJ (1990) Antiepileptic drugs: pharmacological mechanisms and clinical efficacy with consideration of promising developmental stage compounds. *Pharmacol Rev* **42:**223–286.
Steiner TJ, Silveira C, Yuan AWC, and the North Thames Lamictal Study Group (1994) Comparison of lamotrigine (Lamictal) and phenytoin in newly diagnosed epilepsy. *Epilepsia* **35**(suppl 7)**:**61.
West JW, Patton DE, Scheuer T, Wang Y, Goldin AL, and Catterall WA (1992) A cluster of hydrophobic amino acid residues required for fast Na^+ channel inactivation. *Proc Natl Acad Sci USA* **89:**10910–10914.
Willow M, Gonoi T, and Catterall WA (1985) Voltage clamp analysis of the inhibitory actions of diphenylhydantoin and carbamazepine on voltage-sensitive sodium channels in neuroblastoma cells. *Mol Pharmacol* **27:**549–558.
Xie XM, Lancaster B, Peakman T, and Garthwaite J (1995) Interaction of the antiepileptic drug lamotrigine with recombinant rat brain type IIA Na^+ channels and with native Na^+ channels in rat hippocampal neurons. *Pflugers Arch - Eur J Physiol* **430:**437–446.
Zimmerman JJ and Feldman S (1989) Physical-chemical properties and biological activity, in *Principles of Medicinal Chemistry*, ed 3 (Foye WO, ed), pp 7–37, Lea & Febiger, Malvern, PA.

Send reprint requests to: Dr. Chung-Chin Kuo, Department of Physiology, National Taiwan University College of Medicine, No. 1, Jen-Ai Road, 1st Section, Taipei, 100, Taiwan, Republic of China. E-mail: ckuo@ha.mc.ntu.edu.tw